Electronic Supplementary Material (ESI) for Nanoscale.

Supporting information

Diameter-dependent single- and double-file stacking of squaraine dye molecules inside chirality-sorted single-wall carbon nanotubes

Salomé Forel,[a†] Han Li,[b*] Stein van Bezouw,[a] Jochen Campo,[a] Laura Wieland,[b,c] Wim Wenseleers,[a*] Benjamin S. Flavel,[b*] Sofie Cambré[a*]

[a]Nanostructured and Organic Optical and Electronic Materials, Physics Department, University of Antwerp, Belgium.

[b]Institute of Nanotechnology, Karlsruhe Institute of Technology, Hermann-von-Helmholtz-Platz 1, Eggenstein-Leopoldshafen, 76344, Germany.

[c]Institute of Materials Science, Technische Universität at Darmstadt, Alarich-Weiss-Straße 2, Darmstadt, 64287, Germany

†Current address: Université Claude Bernard Lyon 1, UMR CNRS 5615, Lyon, France

*corresponding authors: han.li@kit.edu, wim.wenseleers@uantwerp.be, benjamin.flavel@kit.edu and sofie.cambre@uantwerpen.be

Table of Contents:

S1. Absorption spectra

Figure S1 presents the absorption spectra of the parent samples after metallic/semiconducting sorting and before chiral sorting. These parent samples are prepared both for squaraine-filled SWCNTs, and for non-filled SWCNTs. Figure S2 presents the (14,6)-sorted SWCNT samples, either empty, water-filled, squaraine-filled and alkane-filled to verify that the squaraine-filled SWCNTs present a different electronic shift with respect to the empty or water-/alkane-filled SWCNTs. Figure S3 then zooms in on the dye-absorption band observed within the different chirality-sorted SWCNT samples, showing this dye absorption band comprises contributions from different narrower peaks. Figure S4 shows that when starting from small diameter SWCNT samples, like the CoMoCat (6,5) SWCNT samples which have a narrow diameter distribution centered around the (6,5) SWCNTs, the dye cannot be encapsulated, while larger diameter SWCNT samples like the Electric Arc P2 samples, used throughout this work, or Tuball SWCNTs do get filled with the dye molecule. Moreover, this figure also demonstrates the efficiency of removing externally adsorbed dye molecules by our applied rinsing procedure, as no signature of squaraine is present in the CoMoCat (6,5) sample after the same refluxing in a saturated solution of the dye and rinsing has been applied as for the other samples studied in this work.

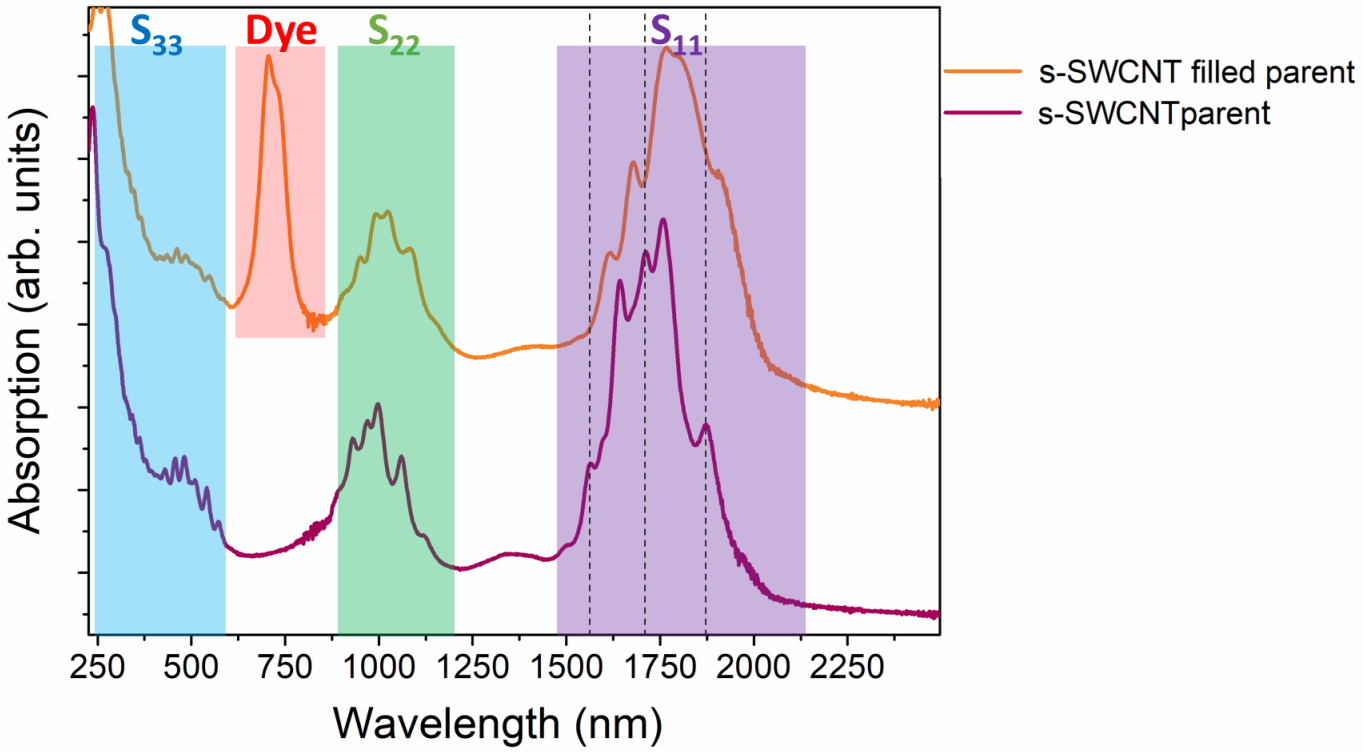

Figure S1. Absorption spectra of the SQ-filled and non-filled semiconducting parent samples clearly demonstrating the dye absorption in the range of 680-800 nm, where no SWCNT transitions are present in the semiconducting parent sample. Moreover, also shifts and line width changes of the intrinsic SWCNT transitions can be clearly observed after dye-filling.

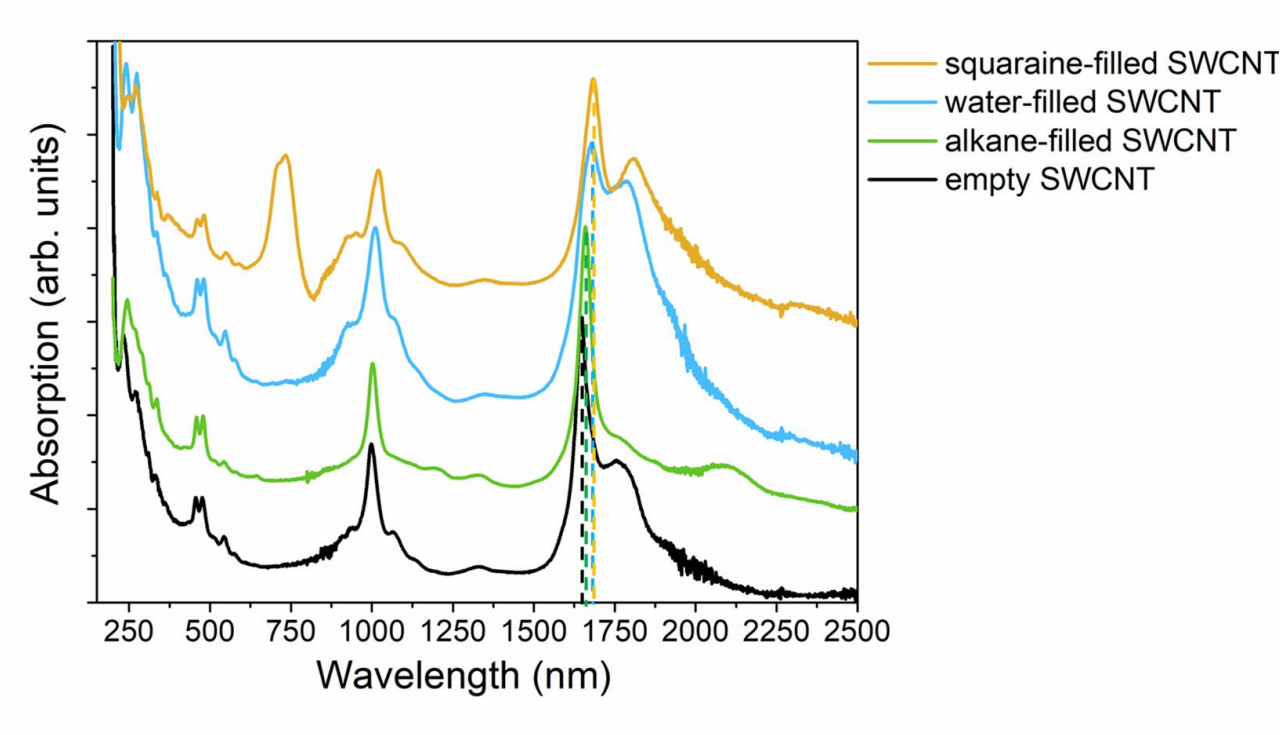

Figure S2. Absorption spectra of the chirality-sorted (14,6) samples comparing different endohedral contents (and showing slightly different chiral purities). Note that slightly different purities are obtained in the different filled samples, when using the exact same chiral sorting procedure.

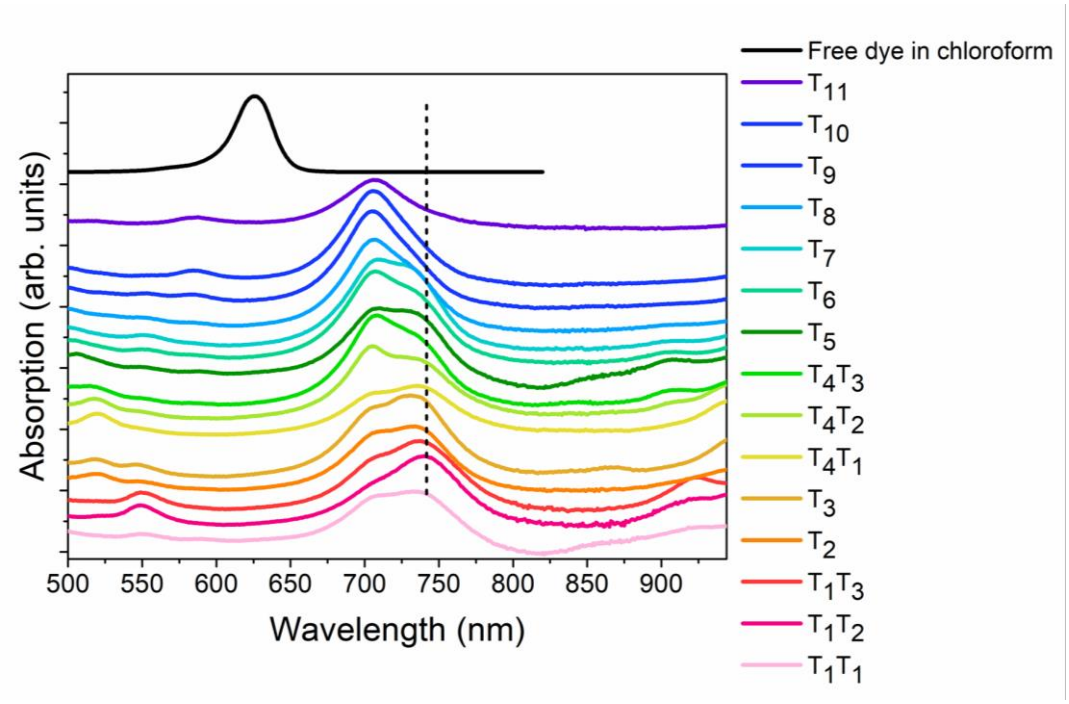

Figure S3. Absorption spectra of the free dye in a chloroform solution (in black) and the same spectra as in Figure 1, zoomed in on the region of the dye absorption in different chirality-sorted SQ@SWCNT samples.

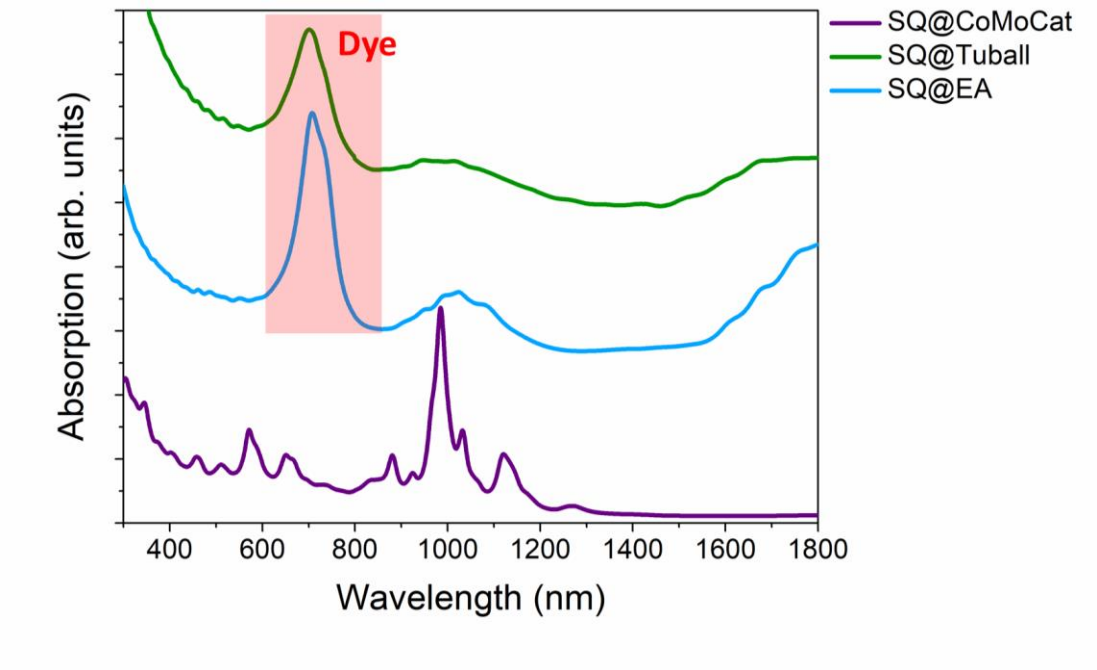

Figure S4. Absorption spectra after SQ filling procedure of different SWCNT samples with different diameter distributions.

S2. Experimental PLE spectra

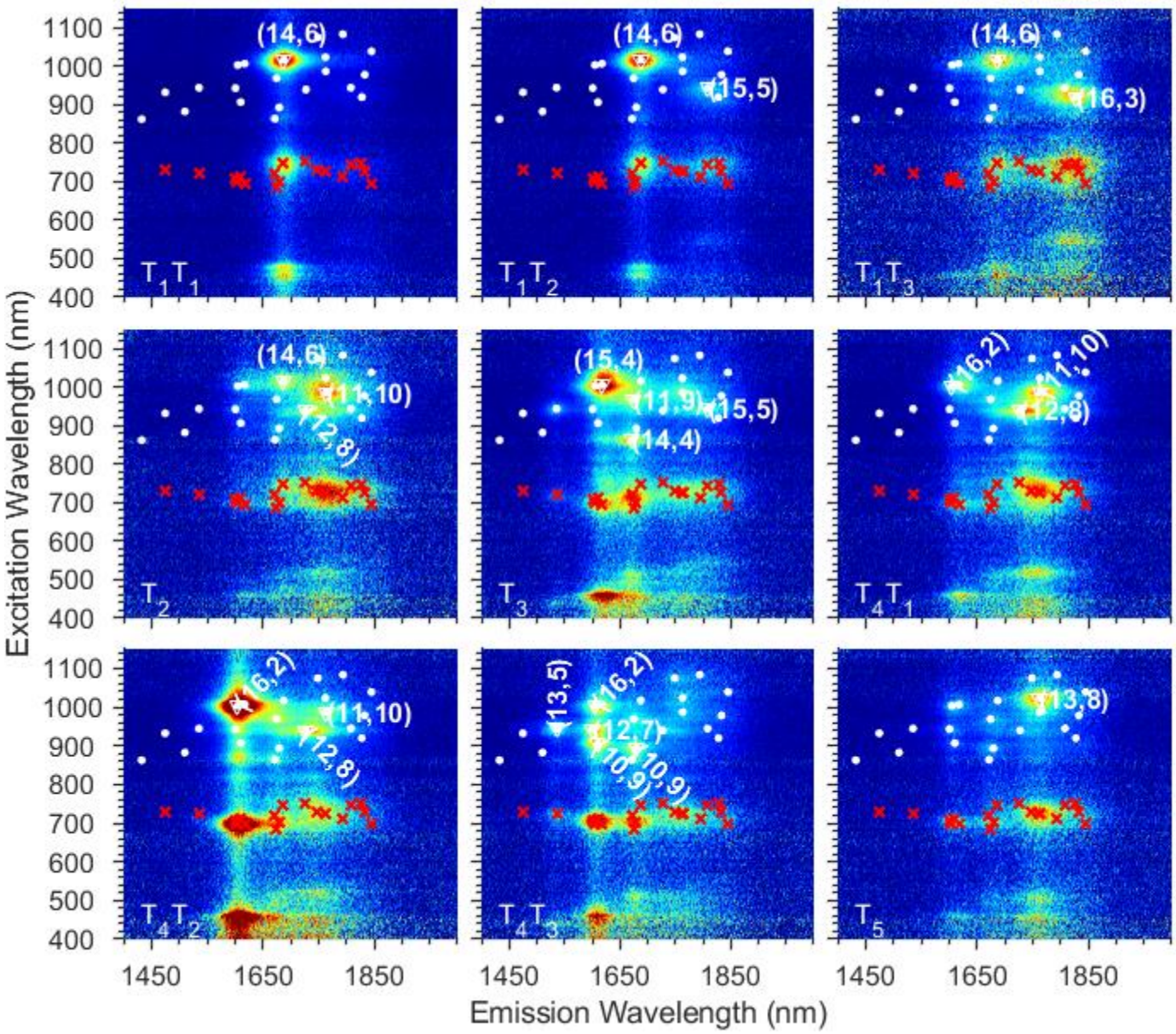

Figure S5. Continued on next page

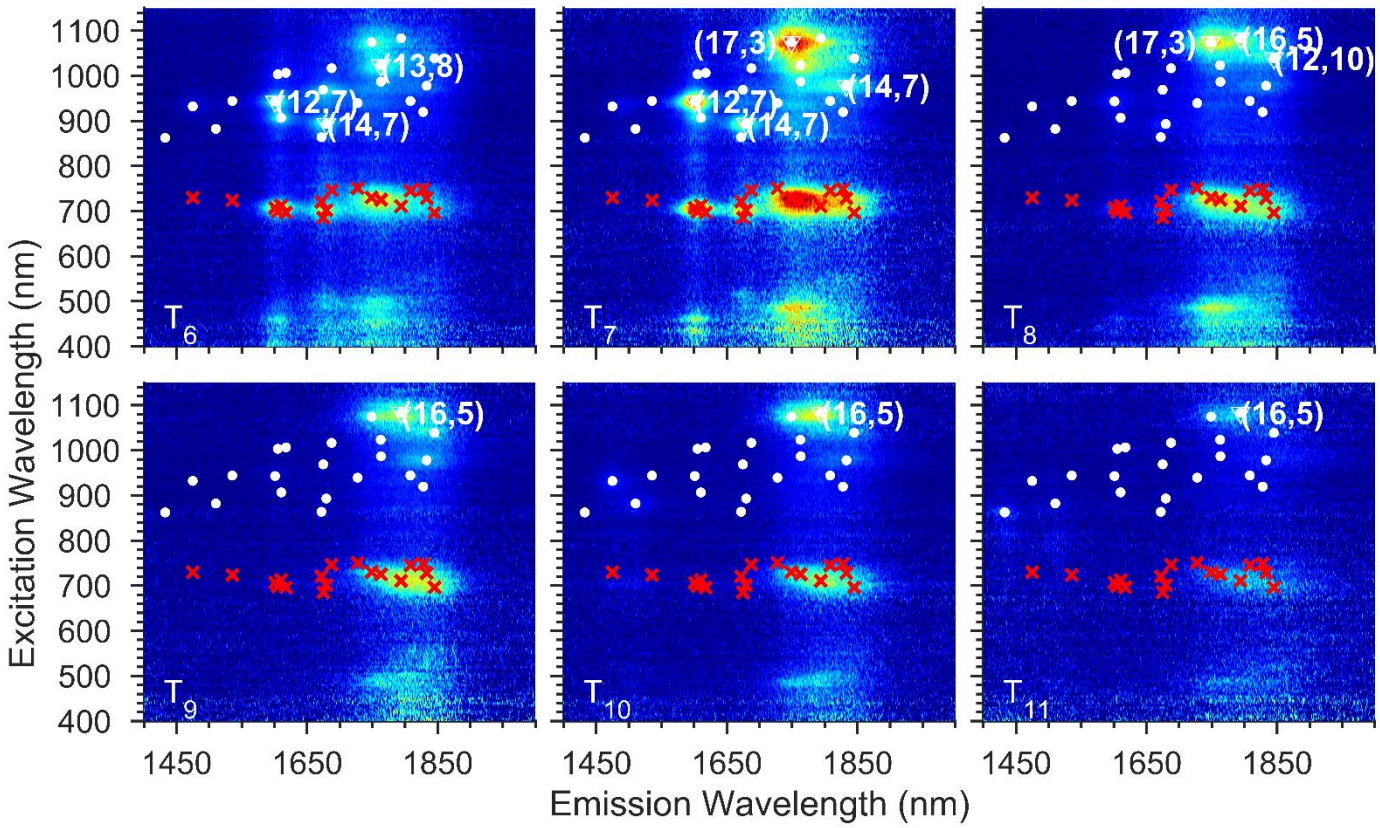

Figure S5. 2D experimental PLE maps of all the SQ-filled and chirality-sorted SWCNT samples. The white dots represent the peak positions of all the chiralities that have been fitted and the red crosses highlight the corresponding fitted EET peak positions. The most abundant chiralities in each map are labelled with their chiral indices and surrounded by a white triangle.

S3. Fits of all the PLE spectra

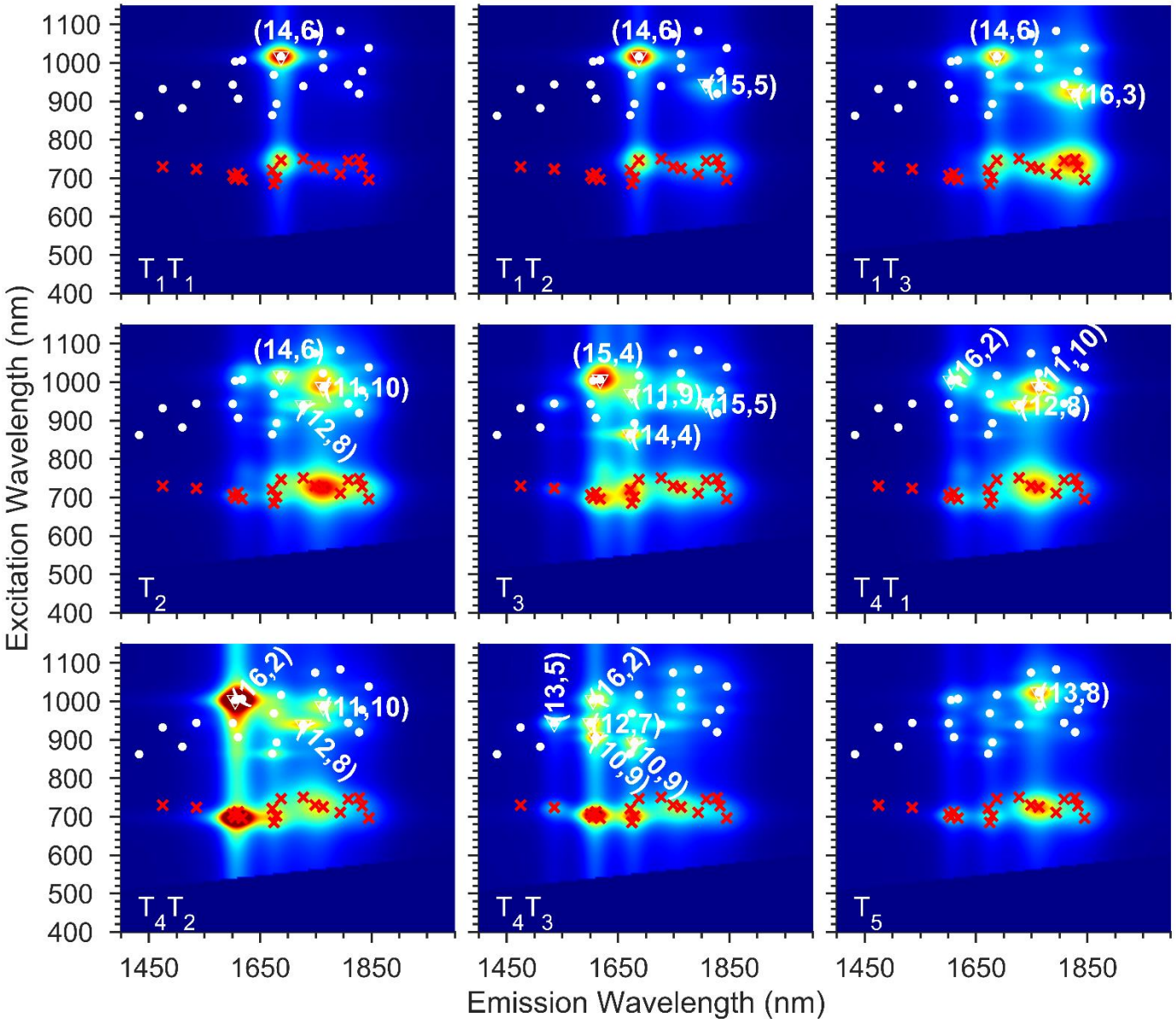

Figure S6. Continued on next page

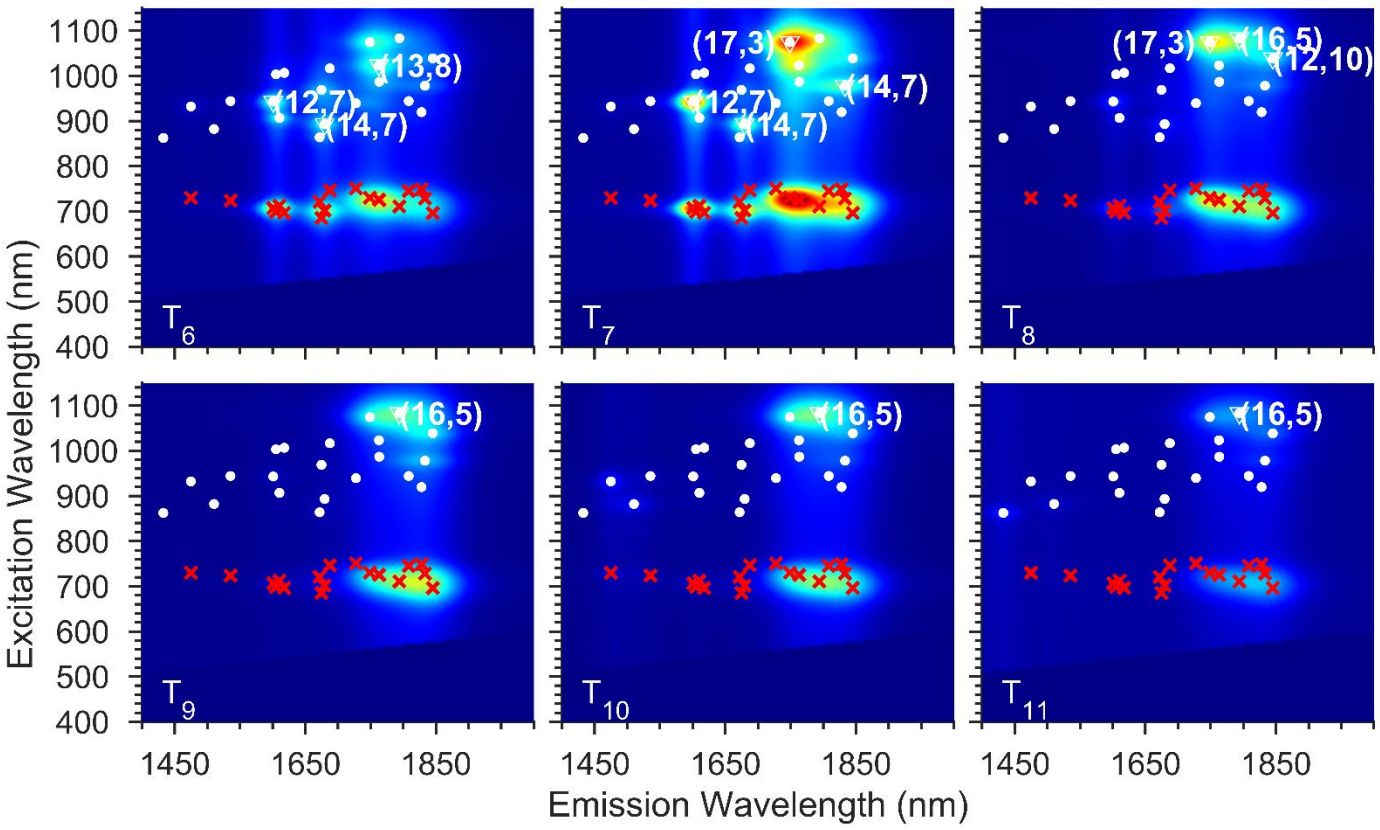

Figure S6. 2D fitted PLE maps of SQ filled SWCNTs, corresponding to the experimental data shown in Figure S5. The white dots represent the peak positions of all the chiralities that have been fitted and the red crosses highlight the corresponding fitted EET peak positions. The most abundant chiralities in each map are labelled with their chiral indices and surrounded by a white triangle.

S4. Model for the EET peak in the fit

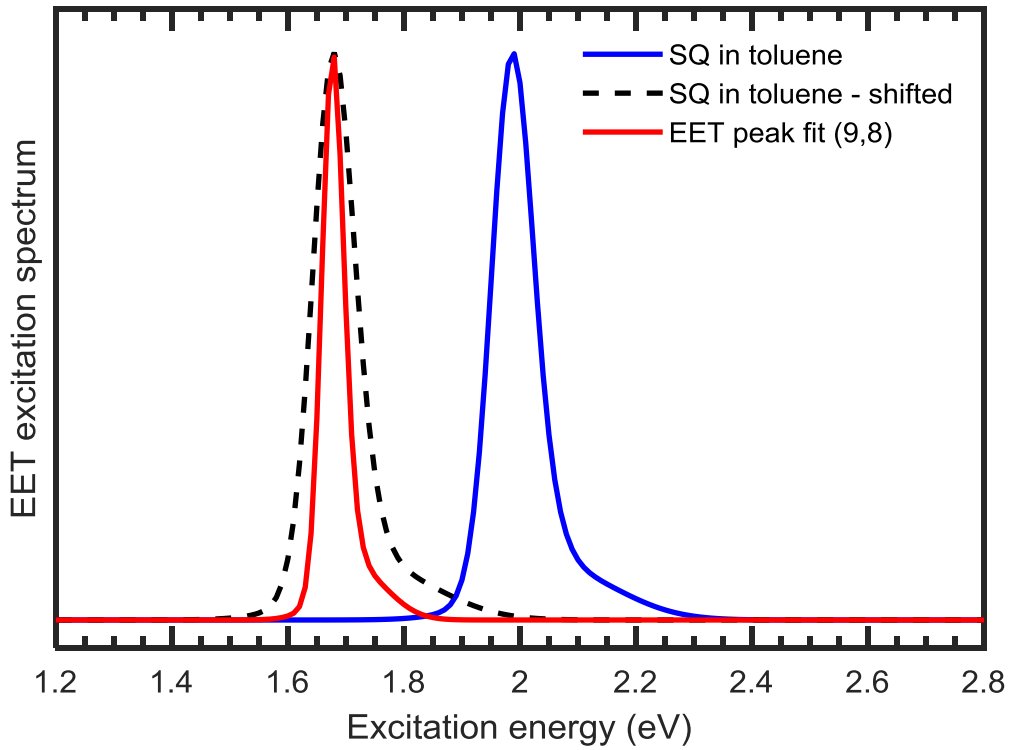

Figure S7: Fitted EET excitation spectrum (red) for the (9,8) chirality, as obtained from the 2D fit. We present the measured absorption spectrum of SQ in toluene (blue line), shifted it to the EET position of the (9,8) chirality (black dashed line) and subsequently scaled it to a narrower line width (red line). The scaling factor, represented in the main text as the EET line width factor, is optimized during the fit for each separate chirality and can be both narrower or broader than 1.

S5. Refit of previous work

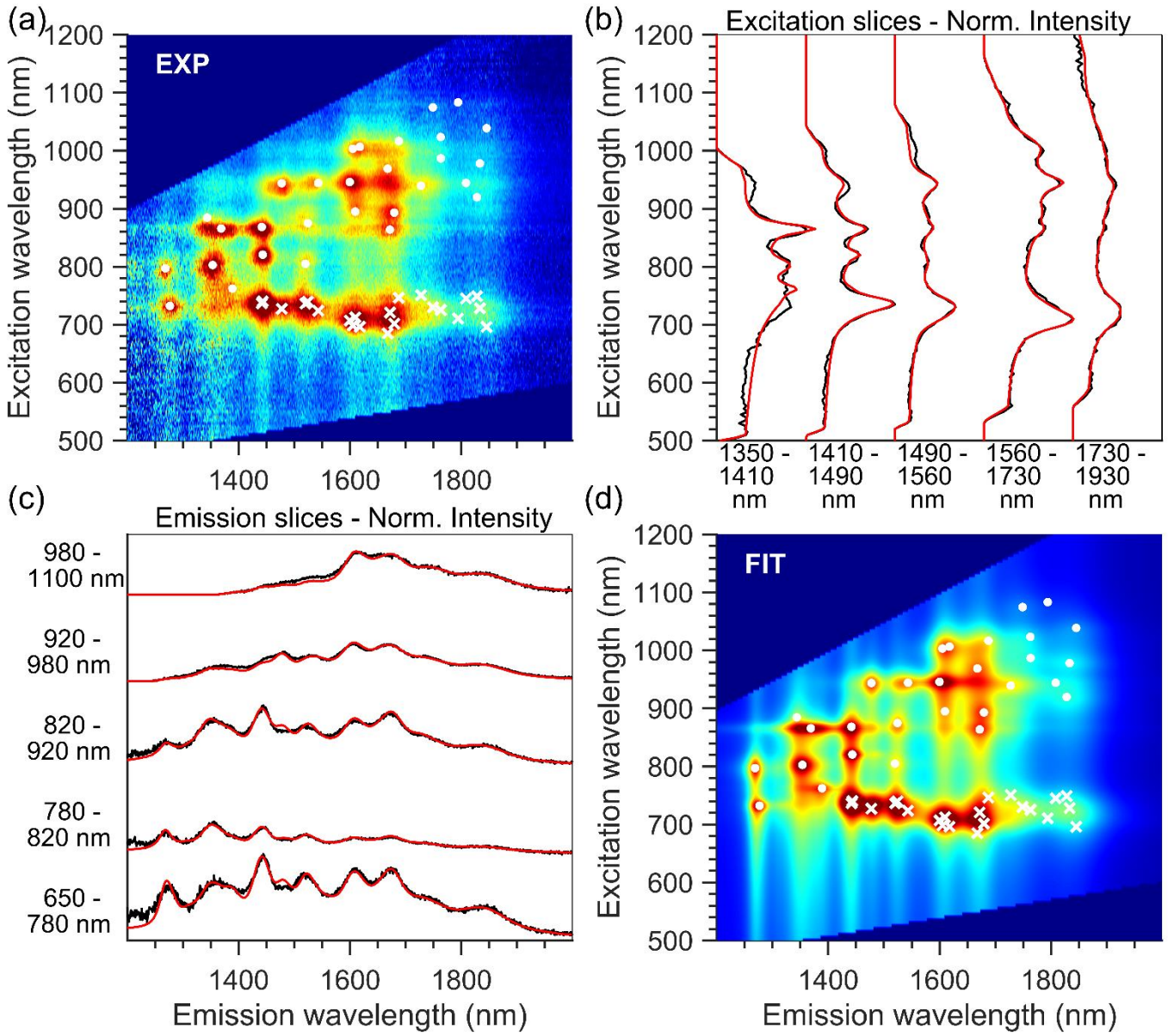

Figure S8. Fit for the PLE map of the sample from previous work [25]: (a) Experimental data. (b) Excitation slices of the experimental spectra (black) and fits (red) taken between the emission wavelengths as indicated below each slice. (c) Emission slices (same color coding) taken between the excitation wavelengths as indicated next to each slice and (d) Fitted PLE map. Peak positions of all fitted SWCNT chiralities and respective EET peaks are presented by white dots and crosses, respectively, in panels (a) and (d).

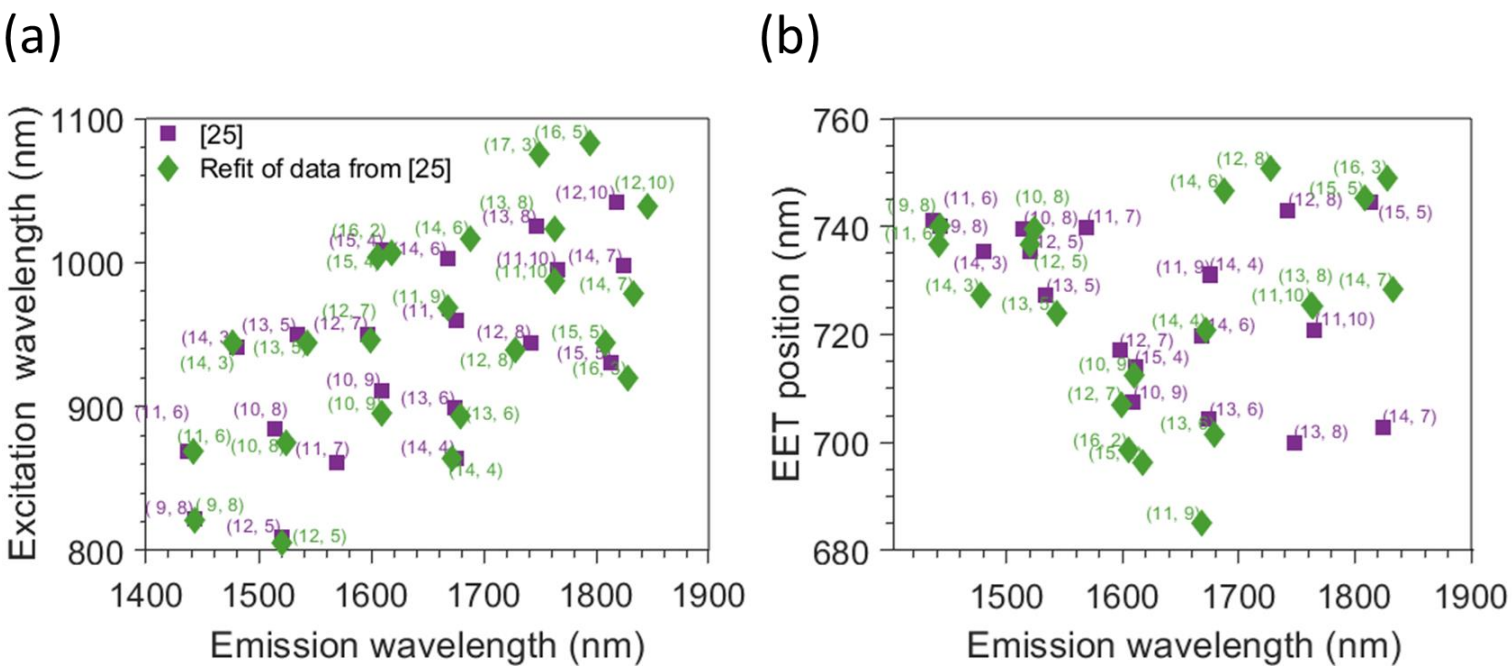

Figure S9. (a) EET peak positions and (b) intrinsic SWCNT peak positions of squaraine-dye-filled SWCNTs, extracted from the new analysis of the data from ref [25] using the optimized fit code that allows for fitting the line width of the EET peaks (and fitting all the chirality-sorted SWCNT samples simultaneously).

S6. Model for dye interaction in a 1D array inside SWCNTs

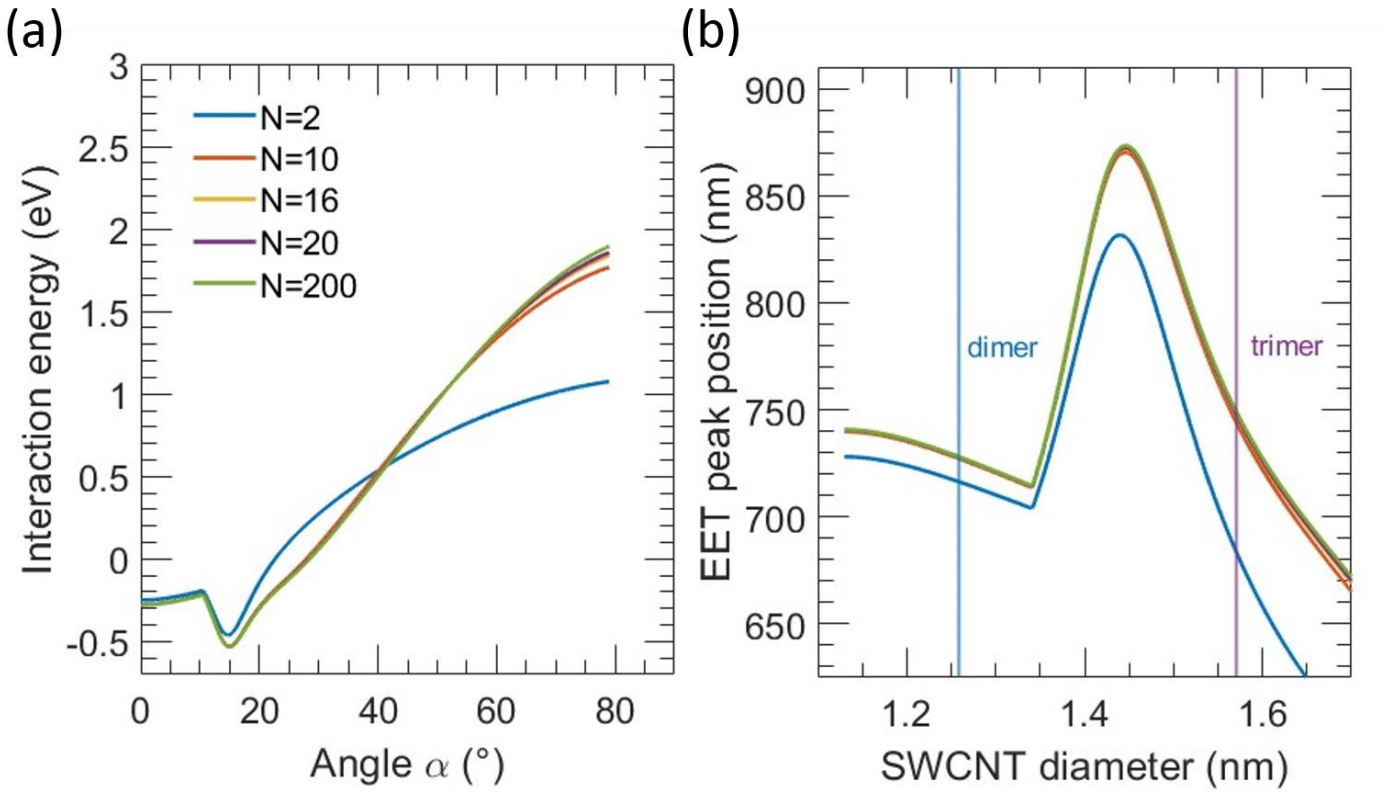

Figure S10 **(a)** Calculated interaction energy as a function of the angle between molecules for an array of N molecules to verify that for *N*=200 the value of an infinite chain is approached (hardly any difference between *N*=20 and *N*=200 in the relevant range (angles < 40 degrees) **(b)** Calculated EET peak position as a function of the nanotube diameter for an array of *N* molecules.